Albino seedling lethality 4 ; chloroplast 30S ribosomal protein S1 required for chloroplast ribosome biogenesis and early chloroplast development in rice

Kunneng Zhou
Anhui Academy of Agricultural Sciences https://orcid.org/0000-0003-4059-5371
Caijuan Zhang
Anhui Academy of Agricultural Sciences
Jiafa Xia
Anhui Academy of Agricultural Sciences
Peng Yun
Anhui Academy of Agricultural Sciences
Yuanlei Wang
Anhui Academy of Agricultural Sciences
Tingchen Ma
Anhui Academy of Agricultural Sciences
Zefu Li (lizefu@aliyun.com)
Anhui Academy of Agricultural Sciences https://orcid.org/0000-0003-3949-1719

Original article

Keywords: chloroplast rRNAs, Oryza sativa, plastid-encoded genes, plastid ribosomal proteins, plastid transcription, 30S ribosomal protein S1

Posted Date: April 2nd, 2021

DOI: https://doi.org/10.21203/rs.3.rs-367189/v1

Albino seedling lethality 4; chloroplast 30S ribosomal protein S1 required for chloroplast ribosome biogenesis and early chloroplast development in rice

Kunneng Zhou[a], Caijuan Zhang[a], Jiafa Xia, Peng Yun, Yuanlei Wang, Tingchen Ma, Zefu Li*

*Correspondence: lizefu@aliyun.com

[a]Kunneng Zhou and Caijuan Zhang contributed equally to this work.

Anhui Province Key Laboratory of Rice Genetics and Breeding (Rice Research Institute, Anhui Academy of Agricultural Sciences), Hefei 230031, China

Abstract

Background: Ribosomes responsible for transcription and translation of plastid-encoded proteins in chloroplasts are essential for chloroplast development and plant growth. Although most ribosomal proteins in plastids have been identified, the molecular mechanisms regulating chloroplast biogenesis remain to be investigated.

Results: Here, we identified albinic seedling mutant *albino seedling lethality 4* (*asl4*) caused by disruption of 30S ribosomal protein S1 that is targeted to the chloroplast. The mutant was defective in early chloroplast development and chlorophyll (Chl) biosynthesis. A 2,855-bp deletion in the *ASL4* allele was verified as responsible for the mutant phenotype by complementation tests. Expression analysis revealed that the *ASL4* allele was highly expressed in leaf 4 sections and newly expanded leaves during early leaf development. Expression levels were increased by exposure to light following darkness. Some genes involved in chloroplast biogenesis were up-regulated and others down-regulated in *asl4* mutant tissues compared to wild type. Plastid-encoded plastid RNA polymerase (PEP)-dependent photosynthesis genes and

nuclear-encoded phage-type RNA polymerase (NEP)-dependent housekeeping genes were separately down-regulated and up-regulated, suggesting that plastid transcription was impaired in the mutant. Transcriptome and western blot analyses showed that levels of most plastid-encoded genes and proteins were reduced in the mutant. The decreased contents of chloroplast rRNAs and ribosomal proteins indicated that chloroplast ribosome biogenesis was impaired in the *asl4* mutant.

Conclusions: Rice *ASL4* encodes 30S ribosomal protein S1, which is targeted to the chloroplast. *ASL4* is essential for chloroplast ribosome biogenesis and early chloroplast development. These data will facilitate efforts to further elucidate the molecular mechanism of chloroplast biogenesis.

Keywords: chloroplast rRNAs, *Oryza sativa*, plastid-encoded genes, plastid ribosomal proteins, plastid transcription, 30S ribosomal protein S1

Background

Plastids have their own genome and transcriptional and translational systems. Plastid ribosomes are the main sites of plastid protein translation in higher plants. Nearly 120 proteins are translated in plastid ribosomes (Hiratsuka et al. 1989). In common with prokaryotes plastid ribosomes are composed of 50S large subunits and 30S small subunits. The large subunit combines 23S and 5S rRNA and contains 33 to 36 proteins. The small subunit consists of 16S rRNA and 21 to 25 proteins (Sharma et al. 2007; Yamaguchi et al. 2000a, b).

Plastid ribosomes have important roles in plastid development and differentiation.

Mutations in genes affecting plastid ribosomes can lead to disrupted embryonic development and albinism that is lethal following exhaustion of energy reserves in the endosperm of the parent seed. Maize PRPS17 was the first reported chloroplast ribosomal protein, mutation in which reduced the translation of plastid proteins and photosynthetic rate causing a light and temperature dependent lethal phenotype (Schultes et al. 2000). In addition, mutation of PRPS9, another member of the same gene family, caused death of the embryo and hence lack of germination (Ma and Dooner 2004; Qiu et al. 2018). Reverse genetics studies showed that chloroplast ribosomal small (PRPS9, 13 and 20) and large (PRPL1, 4, 6, 10, 13, 18, 21, 27, 28, 31 and 35) subunit proteins have essential roles in embryonic development and seed formation in Arabidopsis (Bryant et al. 2011; Hsu et al. 2010; Lloyd and Meinke 2012; Romani et al. 2012; Yin et al. 2012). Knockout of *PRPS2*, *S4*, *S18* and *L20* in tobacco affected protein synthesis and function of chloroplast ribosomes leading to cell death and leaf deformity (Rogalski et al. 2006, 2008). Rice *ASL1* and *ASL2* encode plastid ribosomal small subunit S20 and large subunit L21, respectively; *asl1* and *asl2* mutants suppressed chloroplast development and caused albinic seedlings (Gong et al. 2013; Lin et al. 2014). Loss of function of RPS20 in *E. coli*, the homologous protein of PRPS20, decreased ribosomal activity by modification of 16S rRNA, leading to inhibited assembly of 30s and 50s subunits in forming the 70S ribosome (Aulin et al. 1993). Highly down-regulated expression of 16S rRNA in an *asl1* mutant indicated that PRPS20 in rice has an important role in the accumulation of chloroplast ribosomes (Gong et al. 2013). A single amino acid variation in OsPRPL12 suppressed

67 PEP transcription causing seedling albinism (Zhao et al. 2016).

68 However, not every ribosomal protein is essential for plant growth and development.
69 Although mutations of some plastid ribosomal genes lead to decreased photosynthetic
70 efficiency and plastid protein synthesis they do not prevent whole life processes of the
71 plant. For example, mutations in AtPRPS17, L11 and L24 decrease the synthesis of
72 plastid proteins and photosynthesis, but do not inhibit the basic activity of chloroplast
73 ribosomes (Pesaresi et al. 2001; Romani et al. 2012). Knockout of *PRPL33* showed
74 normal plastid translation and plant growth under natural conditions in tobacco but
75 expressed leaf chlorosis and delayed growth following cold stress (Rogalski et al.
76 2008). *WLP1* was isolated to encode a PRPL13 protein in rice, and a *wlp1* mutant
77 showed a white leaf and panicle phenotype at low temperature (Song et al. 2014).
78 Previous reports suggested that L13 protein had important roles in the folding of 23S
79 rRNA and assembly of 50S ribosomal large subunits (Maguire and Zimmermann
80 2001; Sharma et al. 2007). Loss of function of L13 in *E. coli* caused a lethal
81 phenotype hence differing from the *wlp1* mutant, with an apparently weakened, rather
82 than lethal variation of the *WLP1* gene (Song et al. 2014).

83 Ribosomal protein RPS1 was identified to recognize and bind multiple mRNAs to
84 ribosomes at the initial stage of protein translation in Gram's bacteria (Hajnsdorf and
85 Boni 2012). A T-DNA mutant of *AtPRPS1* obtained by reverse genetics possessed
86 only 8% of the wild-type transcript level, causing leaf chlorosis and delayed plant
87 growth (Romani et al. 2012). Another study showed that PRPS1 interacted with
88 GUN1, and knockout of *GUN1* slowed down the degradation of PRPS1 protein in a

gun1prps1 mutant (Tadini et al. 2016).

In this study, we identified an *asl4* mutant that exhibited an albino seedling phenotype and died after the 3-leaf (L3) stage. The *ASL4* allele encoded 30S ribosomal protein S1 that is targeted to the chloroplast and affects the levels of plastid-encoded genes and proteins. PEP transcription and chloroplast ribosome biogenesis was suppressed in the *asl4* mutant. The data indicated that ASL4 protein is essential for establishment of genetic system during early chloroplast development.

Results

Phenotypic characteristics of the *asl4* mutant

The *asl4* albino mutant (Fig. 1a, b) was identified from a *N*-methyl-*N*-nitrosourea (MNU)-treated population of *Oryza sativa* ssp. *japonica* variety Nongyuan 238. Chl-containing cells were few in number in leaves of the *asl4* mutant compared to wild type (Fig 1c, d). Consistent with the mutant phenotype, the *asl4* mutant could not synthesize Chl and carotenoids (Car) (Fig. 1e). To investigate the effect of the *asl4* mutation on chloroplast development, we examined the ultrastructure of chloroplasts by Transmission electron microscopy (TEM). Wild-type chloroplasts contained well-developed lamellar structures with normally stacked grana and thylakoid membranes (Fig. 1f). In contrast, the *asl4* mutant cells had few and small or undifferentiated chloroplasts with no thylakoid membranes (Fig. 1g-i). These data indicate that *ASL4* plays an essential role in early chloroplast development and plant growth.

Cloning of the *ASL4* gene

The *asl4* mutant was preserved as a heterozygote, the progeny of which segregated 443 normal: 140 albino ($\chi^2_{3:1}$ = 0.302, P_{1df} >0.05), indicating that the *asl4* phenotype was conferred by a single recessive nuclear allele. A segregating F_2 population from a cross of the *asl4* mutant and Nanjing11 was used for gene mapping. The *ASL4* locus was mapped to a 1.03-Mb region between insertion-deletion polymorphic (InDel) markers, C3-16 and K5, on the short arm of chromosome 3 (Fig. 2a). The *ASL4* locus was further delimited to a 50-kb region between markers K40 and K29 using 1,137 albino F_2 individuals (Fig. 2b). Three open reading frames (ORFs) were predicted in the region from the RGAP database (http://rice.plantbiology.msu.edu/cgi-bin/gbrowse/rice/) (Fig. 2c). Sequence analysis demonstrated that the third ORF (*LOC_Os03g20100*) had a 2,855-bp deletion from the 37th bp of intron 4 to the 2,312th bp downstream of the TGA stop codon (Fig. 2d-f). The deletion caused a loss of 96 amino acid residues and added an extra of 29 amino acid residues resulting from the frame-shift translation (Fig S1).

To confirm whether mutation of *ASL4* was responsible for the *asl4* phenotype, an expression vector p*GASL4* containing the entire wild-type *ASL4* genomic DNA was introduced into homozygous *asl4* calli. Marker 'KF' was used to detect transgenic individuals (Fig. 2d; Fig. 3a). All positive plants complemented the *asl4* phenotype whereas the negative controls did not (Fig. 3a, b). These data provided evidence that *LOC_Os03g20100* corresponded to the *ASL4* locus.

ASL4 encodes 30S ribosomal protein S1 that is targeted to the chloroplast

The *ASL4* gene with 7 exons and 6 introns encoding a polypeptide of 402 amino acid

133 residues was predicted to be plastid 30S ribosomal protein S1 (PRPS1) (Fig. 2d, Fig
134 S1). Sequence alignment showed only one copy of ASL4 containing a predicted RNA
135 binding domain covering amino acid residues 254-323 and having extremely high
136 similarity to PRPS1 proteins in other species (Fig S2). The asl4 protein lacked an
137 intact RNA binding domain that presumably disrupted the function of PRPS1 (Fig S1).
138 Phylogenetic analysis showed that PRPS1 orthologs exist in many photosynthetic
139 organisms forming monocot and dicot subclades and likely having evolved from the
140 bryophyta to angiosperms (Fig S3).
141 ASL4 was predicted to be a plastid protein. To determine its localization, free Green
142 fluorescent protein (GFP) and ASL4-GFP fusion plasmid were separately transformed
143 into rice protoplasts. The free GFP was dispersed throughout the cytoplasm (Fig. 4a),
144 whereas ASL4-GFP was merged with Chl autofluorescence (Fig. 4b), hence
145 confirming that ASL4 was a chloroplast protein.
146 **Expression analysis of *ASL4***
147 Expression analysis showed that *ASL4* was constitutively expressed in various rice
148 tissues, with extremely high levels in leaf blades and sheaths (Fig S4). To detect
149 growth stage-specific expression of *ASL4* during leaf development, we analyzed its
150 expression levels in different leaf sections at stage L3. The *ASL4* gene was initially
151 expressed in the shoot base (SB) and the expression levels gradually increased as the
152 L4 developed, and then decreased in L3 tissue, although there was still a high
153 expression level (Fig. 5a, b). This indicated that *ASL4* participated in chloroplast
154 biogenesis.

155 We also measured the *ASL4* transcript in leaf tissues at different seedling development
156 stages. *ASL4* had highest expression levels in newly expanded leaves but levels
157 declined with leaf aging (Fig. 5c). To identify the relationship between *ASL4*
158 expression and light, we detected the *ASL4* accumulation during light-induced
159 greening of wild-type seedlings that had developed in darkness. *ASL4* mRNA levels
160 increased with the extended time of illumination (Fig. 5d), indicating that light might
161 play an important role in regulating *ASL4* expression.

162 **The *asl4* mutant is defective in plastid transcription**

163 Given the effect of *ASL4* mutation on chloroplast development, we examined the
164 expression levels of genes related to chloroplast biogenesis. Compared with the wild
165 type, genes involved in the first (*FtsZ*) and second (*rpoTP2*, *rpoA* and *rpoB*) steps of
166 chloroplast biogenesis were up-regulated in the *asl4* mutant (Fig. 6a), and genes
167 required for the third step (*psaB*, *psbA*, *psbB*, *psbC*, *rbcL*, *rbcS*, *cab1R* and *cab2R*)
168 were down-regulated (Fig. 6b). This suggested that mutation of *ASL4* impeded
169 chloroplast development probably by disrupted expression of genes involved in
170 chloroplast biosynthesis. Down-regulated expression of PEP-dependent
171 photosynthesis genes (such as *psaB*, *psbA* and *rbcL*) and up-regulated NEP-dependent
172 housekeeping genes (*rpoA* and *rpoB*) (Fig. 6a, b) is a typical gene expression pattern
173 resulting from impaired plastid transcription. Messenger-RNA levels of Chl
174 biosynthesis-related genes (*PORA*, *HEMA1*, *YGL1*, *CHLI*, *CHLH* and *CHLD*) were
175 obviously decreased in the *asl4* mutant compared to the wild type (Fig S5).

176 ***ASL4* affects plastid-encoded mRNA and protein levels**

177 To further verify the effect of *ASL4* mutation on plastid transcription, we compared
178 the expression levels of plastid-encoded genes in *asl4* mutant and wild type by
179 transcriptome analysis. Expression of most of the tested plastid-encoded genes was
180 lower in the mutant. The mRNA levels of Class I genes (e.g., *psaA*, *psaB*, *psbA*)
181 transcribed by PEP, including photosystem I (PSI) and photosystem II (PSII), were
182 lower in the *asl4* mutant, whereas Class III genes (e.g., *rpoB*, *rpoC1*) transcribed by
183 NEP including RNA polymerase and ribosomal proteins accumulated (Fig. 7). This
184 was nearly consistent with the results of qPCR (Fig. 6a, b).
185 As ASL4 is a chloroplast ribosomal protein we determined whether mutation of the
186 *ASL4* allele affected the synthesis of plastid-encoded proteins by western blot
187 analyses. The contents of most tested plastid-encoded proteins (psbA, psbB, psbC,
188 psbD, rbcL, AtpB, ndhD and rpoC1) were reduced in *asl4* mutant seedlings (Fig. 8a,
189 d). The increased levels of plastid-encoded proteins rpoA and rpoB might be due to
190 the increased expression of both genes, or accumulated gene product (Fig. 6a; Fig. 7;
191 Fig. 8a, d). The levels of nuclear-encoded proteins, including rbcS, ATPase,
192 RCABP69 and RCA, were lower (Fig. 8b, d). However, the synthesis of
193 mitochondrial-encoded protein, Mt30, was not affected (Fig. 8c, d). Therefore, we
194 inferred that mutation of *ASL4* had a suppressive role in the synthesis of
195 plastid-encoded proteins.
196 **The *asl4* mutant is defective in biogenesis of chloroplast ribosomes**
197 Chloroplast ribosomes are comprised of 50S large subunits and 30S small subunits,
198 and consist of rRNA (5S, 16S and 23S) and ribosomal proteins. To investigate the

changes in chloroplast ribosomes in the *asl4* mutant, we analyzed the components and content of rRNAs using an Agilent 2100 analyzer. The 16S and 23S rRNAs were dramatically decreased in the *asl4* mutant compared to the wild type, whereas the rRNAs in the mitochondrial ribosomes, including 18S and 25S, were not different (Fig. 9a). We also determined that the levels of plastid-encoded ribosomal proteins, including rpl2 (ribosomal protein L2) and rps3 (ribosomal protein S3), were reduced in the *asl4* mutant by western blot analysis (Fig. 9b, c). These results indicated that the biogenesis of chloroplast ribosomes was disrupted in the *asl4* mutant.

Discussion

Several mutants causing albinism or reduced pigment levels have been reported in rice. The mutants have similar phenotypes including decreased pigments levels, suppressed chloroplast biogenesis and early seedling lethality although caused by different genes. Most of the genes affect components of chloroplast ribosomal proteins (Gong et al. 2013; Lin et al. 2014; Zhao et al. 2016). Here, we identified a new chloroplast ribosomal protein ASL4/PRPS1 in rice, mutation of which caused albinism. Sequence analysis showed that the single copy of OsPRPS1 contained a conserved RNA-binding domain (Fig S2; S3). The deleted 2,855 bases resulted in an incomplete RNA-binding domain in PRPS1 (Fig S1). Complementation tests verified that an intact RNA-binding domain was responsible for the wild-type phenotype (Fig. 3a, b). Hence PRPS1 is essential for plant growth and development.

ASL4 transcripts gradually accumulated with elongation of the fourth leaf and reached peak levels in 8-cm L4 leaves at the L3 stage and were also abundant in mature L3

221 leaves (Fig. 5a, b). Previous study showed that the P4 stage of leaf development
222 corresponded to the three steps of chloroplast biogenesis, including plastid division
223 and DNA replication, establishment of the plastid genetic system, and activation of
224 the photosynthetic apparatus (Kusumi et al. 2010). The first step of chloroplast
225 differentiation was almost complete in 2-cm sections of the fourth leaf in which *ASL4*
226 had higher expression levels than the SB (Fig. 5b). The mRNAs of genes *rpoTp* and
227 *rpoA* involved in the second step of chloroplast differentiation highly accumulated
228 before 4-cm sections of the fourth leaf. The *rbcL* and *psbA* transcripts involved in the
229 third step were abundant in the later P4 stage, and peaked at the P5 stage (Kusumi et
230 al. 2011). However, *ASL4* was highly expressed in 2 to 8-cm sections of L4 and the
231 L3 leaf (Fig. 5a, b). These observations suggested that *ASL4* might function
232 throughout all three steps of chloroplast differentiation. We also found that the
233 expression levels of genes associated with the first and second steps of chloroplast
234 biogenesis were up-regulated and genes related to the third step were down-regulated
235 or even not expressed in the *asl4* mutant (Fig. 6a, b). This indicated that chloroplast
236 development was compromised. The reduced mRNA levels of PEP-dependent
237 photosynthesis genes (such as *psaB*, *psbA* and *rbcL*) and increased NEP-dependent
238 housekeeping genes (*rpoA* and *rpoB*) demonstrated that PEP activity was impaired
239 (Fig. 6a, b). This was similar to chloroplast nucleoid-associated protein (Pfalz and
240 Pfannschmidt 2013; Zhong et al. 2013; Zhou et al. 2017). *ASL4* transcripts
241 continuously accumulated with time of illumination during light-induced greening of
242 wild-type seedlings following development in darkness (Fig. 5d), suggesting that

243 synthesis of the chloroplast ribosomal machinery required for light-induced *ASL4*
244 expression (Merendino et al. 2003).
245 Proteins are synthesized in three cell compartments, including cytosol, chloroplast and
246 mitochondria. Nuclear-encoded chloroplast ribosomal proteins, which play essential
247 roles in plastidic protein synthesis, need to be post-translationally targeted to the
248 chloroplasts (Schultes et al. 2000; Song et al. 2014). In this study, ASL4 was
249 identified as nuclear-encoded chloroplast ribosomal protein S1 that affects translation
250 by recognizing and modulating most plastid mRNAs in ribosomes. A deficient RNA
251 binding domain made the S1 protein incapable of binding to the ribosome (Hajnsdorf
252 and Boni 2012). The incomplete RNA binding domain in the *asl4* mutant was
253 similarly defective in protein translation. Most plastid-encoded proteins are similarly
254 severely reduced in the *asl4* mutant (Fig. 8a). However, levels of nuclear-encoded
255 proteins were also reduced (Fig. 8b). Chloroplast development depends on the
256 synergism of nuclear and plastid genes. The status of the chloroplast affects
257 transcription of nuclear genes through retrograde signaling (Nott et al. 2006; Liu et al.
258 2018). The disrupted chloroplast genetic system might therefore restrain the
259 expression and translation of nuclear genes as we found that expression of
260 nuclear-encoded plastid genes was suppressed in the *asl4* mutant (Fig S5).
261 Chloroplast 16S and 23S rRNAs were much reduced in the *asl4* mutant, whereas
262 levels of mitochondrial 18S and 25S rRNAs were unchanged (Fig. 9a). The levels of
263 plastid-encoded ribosomal proteins rpl2 and rps3 were also reduced in the mutant (Fig.
264 9b, c) further inhibiting chloroplast ribosome biogenesis and suppressing synthesis of

plastid proteins.

Arabidopsis PRPS1 affects plant growth and photosynthesis (Romani et al. 2012). A T-DNA insertion mutant of *AtPRPS1* showed pale green leaves and reduced plant size but could complete the entire life cycle. However, our mutant of the PRPS1 in rice led to different results. Although there were similar reductions on plastid proteins (such as PsbA, PsbB and PsbC) in the rice *asl4* mutant and the Arabidopsis T-DNA insertion line, *psbA*, *rbcL* and *psaB* transcripts were up-regulated in Arabidopsis mutant whereas the reverse situation was evident in rice (Fig. 7 and 8; Romani et al. 2012). The effects of homologous PRPS1 in Arabidopsis and rice perhaps differed because 8% of *PRPS1* transcripts in the Arabidopsis mutant formed normal protein. The variation in Arabidopsis *PRPS1* appeared not affect basal ribosome activity, because the 16S and 23S rRNAs were normal in the *AtPRPS1* T-DNA mutant (Romani et al. 2012). However, in this study, we confirmed that OsPRPS1 is essential for plant development.

Conclusions

Rice *ASL4* encodes 30S ribosomal protein S1, which is targeted to the chloroplast. *ASL4* is essential for chloroplast ribosome biogenesis and early chloroplast development. These data will facilitate efforts to further elucidate the molecular mechanism of chloroplast biogenesis.

Materials and methods

Plant materials and growing conditions

The albino seedling *asl4* mutant was obtained from a MNU-treated population of

Oriza sativa spp. *japonica* variety Nongyuan 238. The mutant is maintained as a heterozygote. Plants were grown in a paddy field or a growth chamber. The *asl4* mutant plants were studied from the leaf 2 (L2) to leaf 4 (L4) stage. Selected F_2 populations from a cross between the *asl4* mutant and Nanjing 11 were used to map the *ASL4* locus. For light-induced tests, wild-type seedlings were grown in darkness at 30 ℃ for 10 days, and were then transferred to light for 24 h (30 ℃). Leaf samples were collected every 3 h.

Confocal, determination of photosynthetic pigments and TEM

A number of Chl-containing cells were investigated in leaves of *asl4* mutant and wild type at the L3 stage by confocal laser scanning microscopy (Carl Zeiss LSM700). Fresh leaves for pigment analysis were collected from L2 and L3 leaves of the *asl4* mutant and wild type as described previously (Zhou et al. 2013). Absorbance was measured with a DU 800 UV/Vis Spectrophotometer (Beckman Coulter). Transverse sections of *asl4* mutant and wild-type leaves for transmission microscopy were prepared from L3 stage leaves of seedlings grown in a paddy following methods previously reported (Zhou et al. 2017). The chloroplast ultrastructures were observed with a Hitachi H-7650 transmission electron microscope.

Map-based cloning and complementation test

Ninety two albino individuals from an *asl4* mutant/Nanjing 11 F_2 population were used for linkage analysis. A further 1,137 albino F_2 seedlings were used in fine mapping. New InDel markers were designed with Primer Premier 5.0 based on sequence differences between *indica* and *japonica*. Primers KG-1, KG-2 and KG-3

were used to detect deletions of genomic and cDNA sequences in *asl4* mutant (Suppl. Table S1). Genomic DNAs of three ORFs in the mapping region were amplified and sequenced to detect mutation sites.

For the complementation test, a 6,883-bp genomic sequence of the wild-type *ASL4* allele, including a 2,513-bp upstream sequence, the *ASL4* coding region and a 407-bp downstream sequence, was amplified from Nongyuan 238 and cloned into binary vector pCAMBIA1305 to generate plasmid p*GASL4*, which was then transformed into calli identified as homozygous genotype *asl4asl4*. The empty pCAMBIA1305 vector was also transformed as the control. Marker KF was designed to distinguish positive and negative transgenic plants (Suppl. Table S1).

Bioinformatics analysis and subcellular localization

Candidate genes in the mapping region, sequence information, gene function, and the RNA binding domain of ASL4 were predicted from the RGAP database (http://rice.plantbiology.msu.edu/cgi-bin/gbrowse/rice/). Homologous sequences of the ASL4 protein were identified using NCBI (http://www.ncbi.nlm.nih.gov/) and sequences were aligned using BioEdit software. A neighbor-joining tree based on 1,000 bootstrap replicates was performed with MEGA v4.1 software. The expression profile of *ASL4* gene was predicted with the RiceXPro database (http://ricexpro.dna.affrc.go.jp/).

For subcellular localization, a 1,206-bp coding sequence without the TAG stop codon of the *ASL4* allele was cloned into the N-terminus of GFP in the pA7 vector, which was then transiently transformed into rice protoplasts. The empty vector was similarly

transformed as the control. Fluorescence was observed using the confocal laser scanning microscope (Carl Zeiss LSM700).

Gene expression analysis

Total RNA was extracted using RNA Prep Pure Plant kit (TIANGEN) and reverse-transcribed with a FastKing RT Kit (TIANGEN) according to the manufacturer's instructions. Quantitative RT-PCR was performed using a SYBR_ Premix Ex TaqTM kit (TaKaRa) on an ABI Q3 Real-Time PCR System. Relative gene expression was analyzed using $2^{-\Delta\Delta CT}$ method (Livak and Schmittgen 2001). Primers for quantitative Real-Time PCR were designed by Primer Premier 5.0 or GenScript. The *ubiquitin* gene (ubq) was used as a reference (Suppl. Table S1).

Transcriptome analysis

Total RNA was isolated from L3 seedlings of the *asl4* mutant and wild type. RNA purity was tested with a Nanodrop and RNA integrity and contents of rRNAs were detected by Agilent 2100 analyzer. A library was constructed and sequenced with an lllumina HiSeq 2000 (Novogene). Data were analyzed by the RPKM method (Mortazavi et al. 2008). Plastid-encoded genes were isolated by referring to the chloroplast genome annotation (http://megasun.bch.umontreal.ca/ogmp/projects/other/cp_list.html). Genes with significant differences in expression were determined (*P* value <0.05, $\log_2$ (FoldChange) >1 or <-1).

Western blot analysis

Total proteins were extracted from wild-type and *asl4* mutant seedlings at the L3

353 stage. Tissue samples were ground in liquid nitrogen and isolated with equal volumes
354 of NB1 solution (50 mM Tris-Mes, 0.5 M sucrose, 1 mM $MgCl_2$, 10 mM EDTA, 5
355 mM DTT and protease inhibitor cocktail CompleteMini tablets, pH 8.0) on ice at 20
356 rpm for 30 min. The supernatant was collected by centrifugation at 12,000 rpm for 10
357 min and denatured by adding 5× loading buffer at 95℃ for 5 min. The proteins were
358 separated in SDS-PAGE gels, transferred to polyvinylidene difluoride membranes,
359 and identified with antibodies using an ECL Plus Western Blotting Detection Kit
360 (Thermo). Proteins were quantified by Quantity One software. The relevant antibodies
361 were obtained from BPI (http://www.proteomics.org.cn/).
362
363 **Availability of data and materials**
364 All data supporting the conclusions of this article are provided within the article (and its additional
365 files).
366
367 **Abbreviations**
368 ***asl4*:** *albino seedling lethality 4*
369 **Car:** Carotenoids
370 **Chl:** Chlorophyll
371 **GFP:** Green fluorescent protein
372 **InDel:** Insertion-deletion polymorphic
373 **MNU:** *N*-methyl-*N*-nitrosourea
374 **NEP:** Nuclear-encoded phage-type RNA polymerase
375 **ORF:** Open reading frame
376 **PEP:** Plastid-encoded plastid RNA polymerase
377 **PRPL:** Plastid ribosomal protein large subunit

PRPS: Plastid ribosomal protein small subunit

SB: Shoot base

TEM: Transmission electron microscopy

References

Aulin MR, Zhang SP, Kylsten P, Isaksson LA (1993) Ribosome activity and modification of 16S RNA are influenced by deletion of ribosomal protein S20. Mol Microbiol 7:983–992

Bryant N, Lloyd J, Sweeney C, Myouga F, Meinke D (2011) Identification of nuclear genes encoding chloroplast-localized proteins required for embryo development in Arabidopsis. Plant Physiol 155:1678–1689

Gong XD, Jiang Q, Xu JL, Zhang JH, Teng S, Lin DZ, Dong YJ (2013) Disruption of the rice plastid ribosomal protein S20 leads to chloroplast developmental defects and seedling lethality. Genes Genom Genet 3:1769–1777

Hajnsdorf E, Boni IV (2012) Multiple activities of RNA-binding proteins S1 and Hfq. Biochimie 94:1544–1553

Hiratsuka J, Shimada H, Whittier R, Ishibashi T, Sakamoto M, Mori M, Kondo C, Honji Y, Sun CR, Meng BY (1989) The complete sequence of the rice (*Oryza sativa*) chloroplast genome: intermolecular recombination between distinct tRNA genes accounts for a major plastid DNA inversion during the evolution of the cereals. Mol Gen Genet 217:185–194

Hsu SC, Belmonte MF, Harada JJ, Inoue K (2010) Indispensable roles of plastids in *Arabidopsis thaliana* embryogenesis. Curr Genomics 11:338–349

Kusumi K, Chono Y, Shimada H, Gotoh E, Tsuyama M, Iba K (2010) Chloroplast biogenesis during the early stage of leaf development in rice. Plant Biotechnol 27:85–90

401 Kusumi K, Sakata C, Nakamura T, Kawasaki S, Yoshimura A, Iba K (2011) A plastid protein
402 NUS1 is essential for build-up of the genetic system for early chloroplast development under
403 cold stress conditions. Plant J 68:1039–1050
404 Lin D, Jiang Q, Zheng K, Chen S, Zhou H, Gong X, Xu J, Teng S, Dong Y (2014) Mutation of the
405 rice *ASL2* gene encoding plastid ribosomal protein L21 causes chloroplast developmental
406 defects and seedling death. Plant Biol 17:599–607
407 Liu X, Lan J, Huang Y, Cao P, Zhou C, Ren Y, He N, Liu S, Tian Y, Nguyen T (2018) WSL5, a
408 pentatricopeptide repeat protein, is essential for chloroplast biogenesis in rice under cold
409 stress. J Exp Bot 69: 3949–3961
410 Livak KJ, Schmittgen TD (2001) Analysis of relative gene expression data using real-time
411 quantitative PCR and the $2^{-\Delta\Delta CT}$ method. Methods 25:402–408
412 Lloyd RK, Meinke D (2012) A comprehensive dataset of genes with a loss of function mutant
413 phenotype in Arabidopsis. Plant Physiol 58:1115–1129
414 Ma ZR, Dooner HK (2004) A mutation in the nuclear-encoded plastid ribosomal protein S9 leads
415 to early embryo lethality in maize. Plant J 37:92–103
416 Maguire BA, Zimmermann RA (2001) The ribosome in focus. Cell 104:813–816
417 Merendino L, Falciatore A, Rochaix JD (2003) Expression and RNA binding properties of the
418 chloroplast ribosomal protein S1 from *Chlamydomonas reinhardtii*. Plant Mol Biol
419 53:371–382
420 Mortazavi A, Williams B A, McCue K, Schaeffer L, Wold B (2008) Mapping and quantifying
421 mammalian transcriptomes by RNA-Seq. Nat Methods 5:621–628
422 Nott A, Jung H-S, Koussevitzky S, Chory J (2006) Plastid-to-Nucleus retrograde signaling. Annu

Rev Plant Biol 57:739–759

Pesaresi P, Varotto C, Meurer J, Jahns P, Salamini F, Leister D (2001) Knock-out of the plastid ribosomal protein L11 in Arabidopsis: effects on mRNA translation and photosynthesis. Plant J 27:179–189

Pfalz J, Pfannschmidt T (2013) Essential nucleoid proteins in early chloroplast development. Trends Plant Sci 18:186–194

Qiu Z, Chen D, He L, Zhang S, Yang Z, Zhang Y, Wang Z, Ren D, Qian Q, Guo L (2018) The rice *white green leaf 2* gene causes defects in chloroplast development and affects the plastid ribosomal protein S9. Rice 11: 39

Rogalski M, Ruf S, Bock R (2006) Tobacco plastid ribosomal protein S18 is essential for cell survival. Nucleic Acids Res 34:4537–4545

Rogalski M, Schottler MA, Thiele W, Schulze WX, Bock R (2008) Rpl33, a nonessential plastid-encoded ribosomal protein in tobacco, is required under cold stress conditions. Plant Cell 20:2221–2237

Romani I, Tadini L, Rossi F, Masiero S, Pribil M, Jahns P, Kater M, Leister D, Pesaresi P (2012) Versatile roles of Arabidopsis plastid ribosomal proteins in plant growth and development. Plant J 72:922–934

Schultes NP, Sawers RJ, Brytnell TP, Krueger RW (2000) Maize *high chlorophyll fluorescent 60* mutant is caused by an *Ac* disruption of the gene encoding the chloroplast ribosomal small subunit protein 17. Plant J 21:317–327

Sharma MR, Wilson DN, Datta PP, Barat C, Schluenzen F, Fucini P, Agrawal RK (2007) Cryo-EM study of the spinach chloroplast ribosome reveals the structural and functional roles of

plastid-specific ribosomal proteins. Proc Natl Acad Sci USA 104:19315–19320

Song J, Wei X, Shao G, Sheng Z, Chen D, Liu C, Jiao G, Xie L, Tang S, Hu P (2014) The rice nuclear gene *WLP1* encoding a chloroplast ribosome L13 protein is needed for chloroplast development in rice grown under low temperature conditions. Plant Mol Biol 84:301–314

Tadini L, Pesaresi P, Kleine T, Rossi F, Guljamow A, Sommer F, Mühlhaus T, Schroda M, Masiero S, Pribil M (2016) GUN1 controls accumulation of the plastid ribosomal protein S1 at the protein level and interacts with proteins involved in plastid protein homeostasis. Plant Physiol 170:1817–1830

Yamaguchi K, Knoblauch K, Subramanian AR (2000a) The plastid ribosomal protein. Identification of all the proteins in the 30S subunit of an organelle ribosome (chloroplast). J Biol Chem 275:28455–28465

Yamaguchi K, Subramanian AR (2000b) The plastid ribosomal protein: Identification of all the proteins in the 50S subunit of an organelle ribosome (chloroplast). J Biol Chem 275:28466–28482

Yin T, Pan G, Liu H, Wu J, Li Y, Zhao Z, Fu T, Zhou Y (2012) The chloroplast ribosomal protein L21 gene is essential for plastid development and embryogenesis in *Arabidopsis*. Planta 235:907–921

Zhao D, Zhang C, Li Q, Yang Q, Gu M, Liu Q (2016) A residue substitution in the plastid ribosomal protein L12/AL1 produces defective plastid ribosome and causes early seedling lethality in rice. Plant Mol Biol 91:161–177

Zhong L, Zhou W, Wang H, Ding S, Lu Q, Wen X, Peng L, Zhang L, Lu C (2013) Chloroplast small heat shock protein HSP21 interacts with plastid nucleoid protein pTAC5 and is

essential for chloroplast development in Arabidopsis under heat stress. Plant Cell 25:2925–2943

Zhou K, Ren Y, Lv J, Wang Y, Liu F, Zhou F, Zhao S, Chen S, Peng C, Zhang X (2013) *Young Leaf Chlorosis 1*, a chloroplast-localized gene required for chlorophyll and lutein accumulation during early leaf development in rice. Planta 237:279–292

Zhou K, Ren Y, Zhou F, Wang Y, Zhang L, Lyu J, Wang Y, Zhao S, Ma W, Zhang H (2017) *Young Seedling Stripe 1* encodes a chloroplast nucleoid-associated protein required for chloroplast development in rice seedlings. Planta 245:45–60

Funding

This work was supported by the National Natural Science Foundation of China (31801331), the Key R&D Program of Anhui Province (912167100062), and the National Key R&D Program of China (2016YFD0100101-06, 2017YFD0100406).

Authors' contributions

KZ, JX, and ZL designed the research, performed the experiments, analyzed the data, and wrote the manuscript. CZ, PY, YW, and TM performed the experiments and analyzed the data. All authors read and approved the final manuscript.

Ethics approval and consent to participate

There are no ethical issues associated with this article.

Consent for publication

All co-authors give consent to publish this article in *Rice*.

Competing interests

The authors declare that they have no competing interests.

Publisher's Note

Springer Nature remains neutral with regard to jurisdictional claims in published maps and institutional affiliations.

Acknowledgements

Not applicable

Author details

Anhui Province Key Laboratory of Rice Genetics and Breeding (Rice Research Institute, Anhui Academy of Agricultural Sciences), Hefei 230031, China

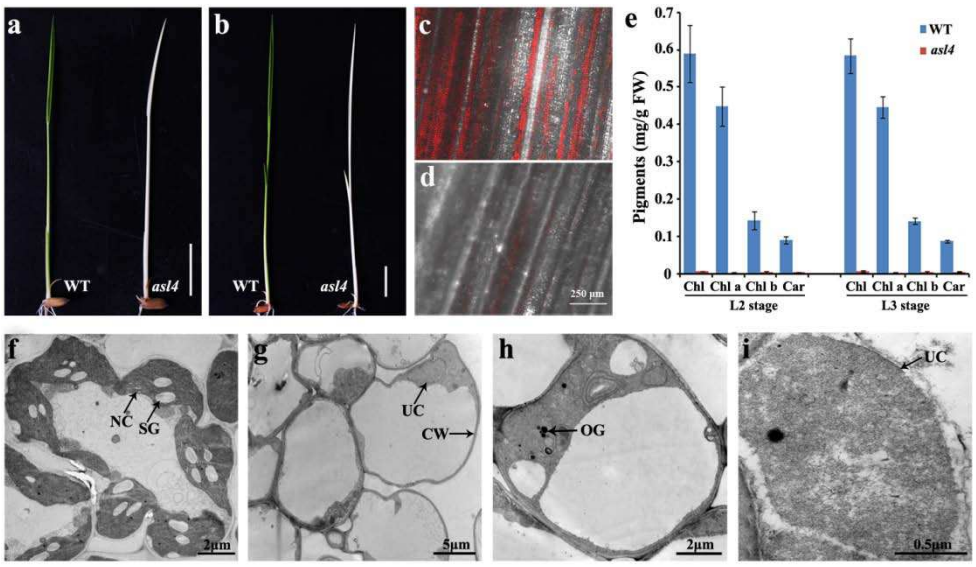

Figure 1 Phenotypic characteristics of the *asl4* mutant. **a** Phenotype of wild type and the *asl4* mutant at the L2 stage grown in the field. **b** Phenotype of wild type and the *asl4* mutant at the L3 stage. Confocal microscope observation of chlorophyll-containing cells in seedlings of wild type (**c**) and the *asl4* mutant (**d**). **e** Photosynthetic pigment determination in seedlings of wild type and *asl4* mutant at the L2 and L3 stages. Values are means ± SD from three independent replicates. TEM observations of chloroplasts in wild type (**f**) and *asl4* (**g**-**i**) seedlings at the L3 stage. *NC* normal chloroplast, *SG* starch granule, *UC* undifferentiated chloroplast, *CW* cell wall, *OG* osmiophilic plastoglobuli

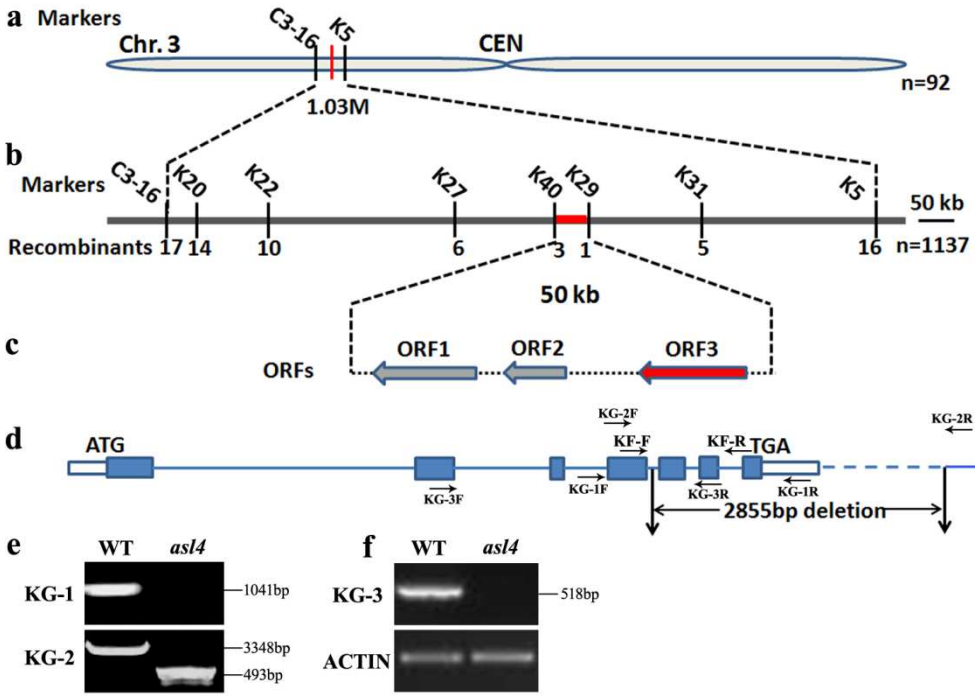

Figure 2 Map-based cloning of the *ASL4* locus. **a** The *ASL4* locus was initially mapped to a 1.03-Mb region between markers C3-16 and K5 on the short arm of chromosome 3. **b** *ASL4* was fine-mapped to a 50-kb region between markers K40 and K29 using 1,137 F_2 mutant seedlings. **c** Three ORFs were predicted in the region. **d** Structure of *ASL4*. ATG and TGA indicate start and stop codons. *Blue boxes* indicate exons and the lines between them indicate introns. *White boxes* represent the 5' and 3' UTR. The location of the 2,855-bp deletion in the *asl4* allele is indicated. PCR identification of genomic DNAs (**e**) and cDNA (**f**) between wild type and *asl4* mutant using primer pairs indicated in D. The *actin* gene was amplified as the control.

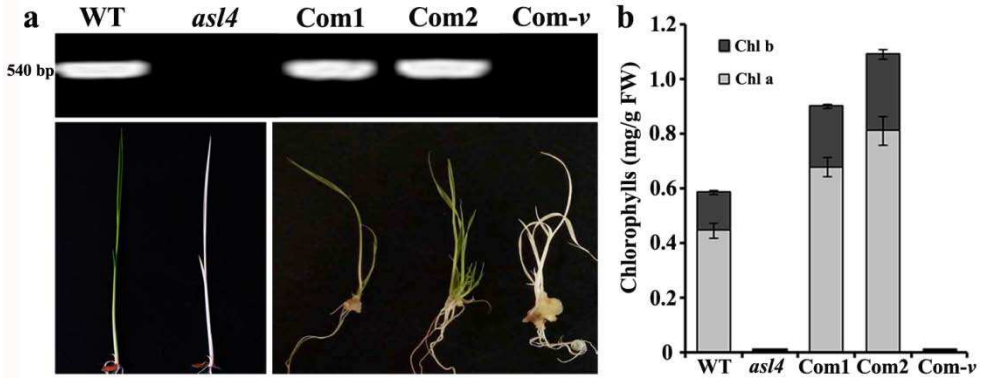

Figure 3 Complementation test of the *asl4* mutation. **a** Phenotypes of wild type, *asl4* mutant and transgenic plants. Primer KF indicated in figure 2D was used to distinguish positive and negative lines. **b** Chlorophyll contents of wild type, *asl4* mutant and transgenic plants. Values are means ± SD from three independent repeats. Com1, Com2 and Com-v are two positive transgenic lines and transformation control with empty vector, respectively.

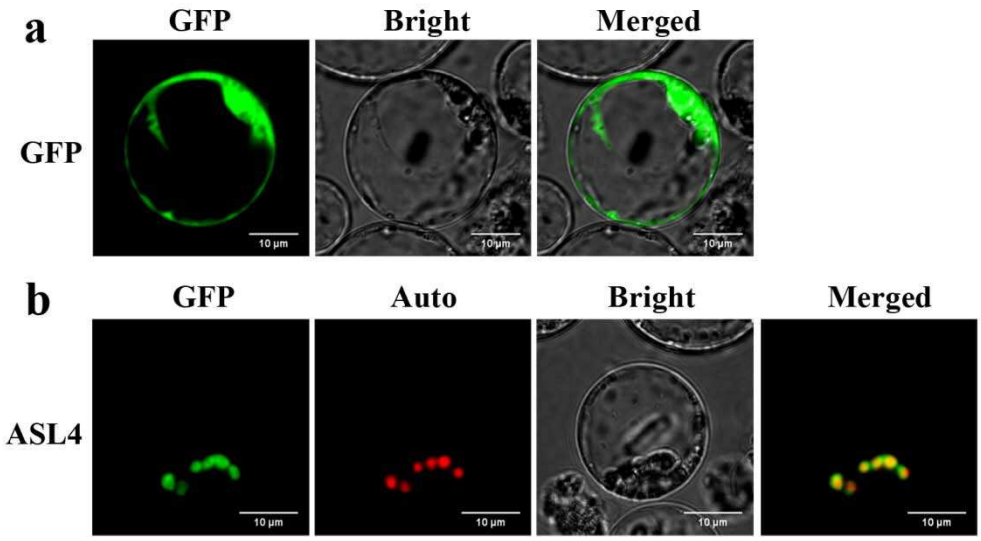

Figure 4 Subcellular location of ASL4 protein. **a** Free GFP signals in rice protoplasts. **b** ASL4-GFP signals were co-localized with chlorophyll autofluorescence in rice protoplasts. GFP, GFP signals of free GFP and ASL4; Auto, chlorophyll autofluorescence; Bright, bright field; Merged, merged images.

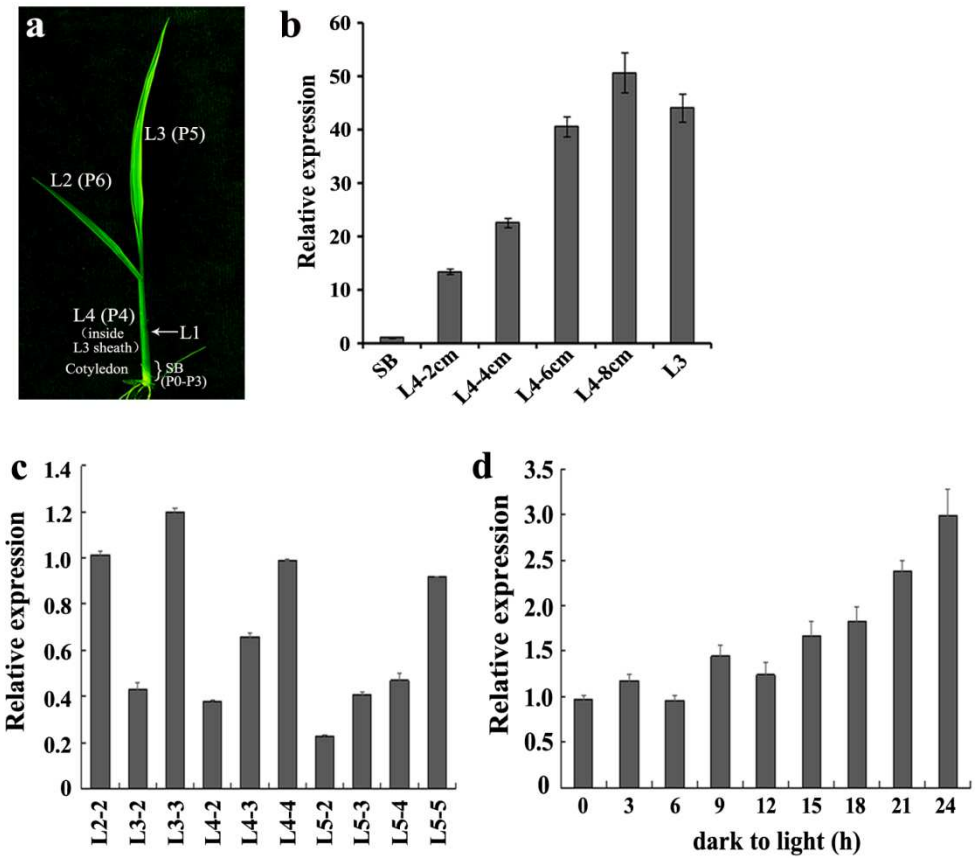

Figure 5 Expression analysis of *ASL4*. **a** Diagram of a L3 stage seedling when leaf 3 is fully expanded. SB (shoot base) indicates a 5 mm piece from the bottom of the shoot. L1-L4 represent leaves 1 to 4 in the L3 stage seedling. P0-P6 represent the developmental stages of leaf formation. **b** Expression of *ASL4* in different wild-type sections at the L3 stage seedling from the paddy field. L4-2 cm, 4 cm, 6 cm and 8 cm indicate the length of the L4 leaf. **c** Expression levels of *ASL4* in wild-type leaves at different stages. For example, L2-2 represent leaf 2 of a L2 stage seedling, L3-2 represent leaf 2 of a L3 stage seedling. **d** Expression analysis of *ASL4* during light-induced greening of wild-type seedlings. Wild-type seedlings were exposed to light for 3h, 6h, 9h, 12h, 15h, 18h, 21h and 24h after 10 days of growth at 30℃in darkness. The *ubiquitin* gene was used as internal control. Values are means ± SD from three independent replicates.

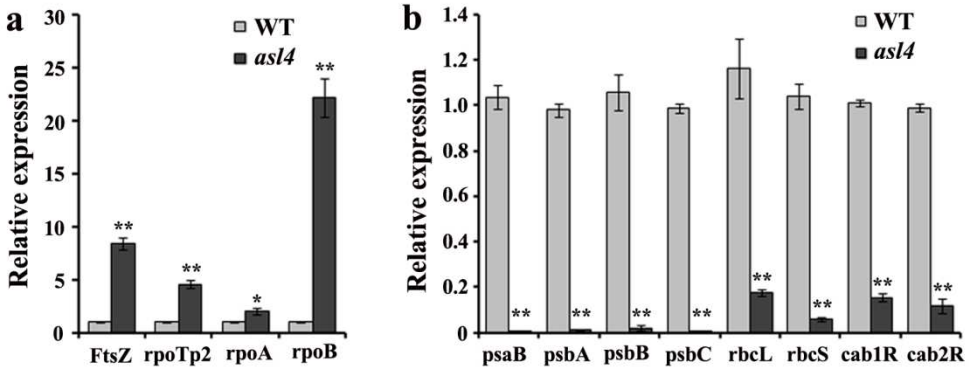

Figure 6 Expression levels of genes involved in chloroplast biogenesis. Expression levels of genes associated with the first and second (**a**) and third (**b**) steps of chloroplast biogenesis in wild-type and *asl4* mutant seedlings at the L3 stage. Data are means ± SD of three independent repeats. ** and *, indicate significance at $P = 0.01$ and $P = 0.05$, respectively, by Student's *t* tests.

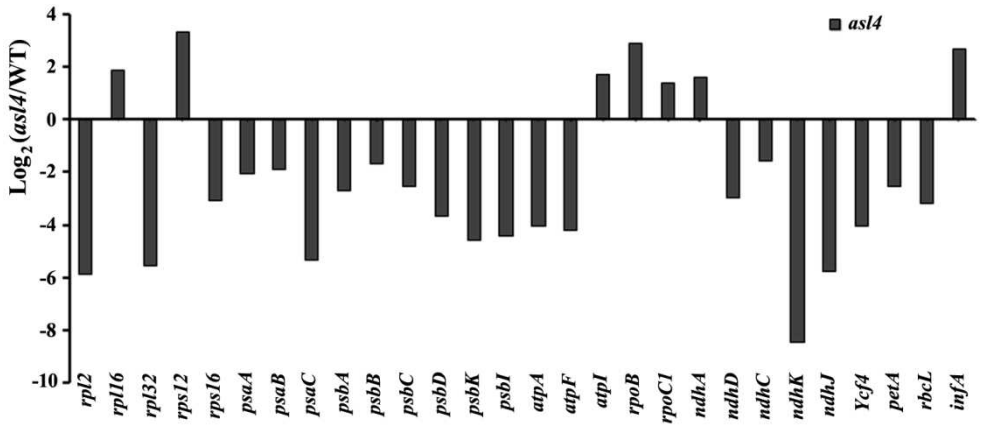

Figure 7 Transcripts of plastid-encoded genes detected by transcriptome analysis. Total RNA was isolated from wild-type and *asl4* mutant seedlings at the L3 stage and reverse-transcribed by random hexamer primers. The library was constructed and sequenced with an lllumina HiSeq 2000. Log_2 (*asl4*/WT) indicates the log_2 ratio of mRNA levels in *asl4* mutant compared to wild type.

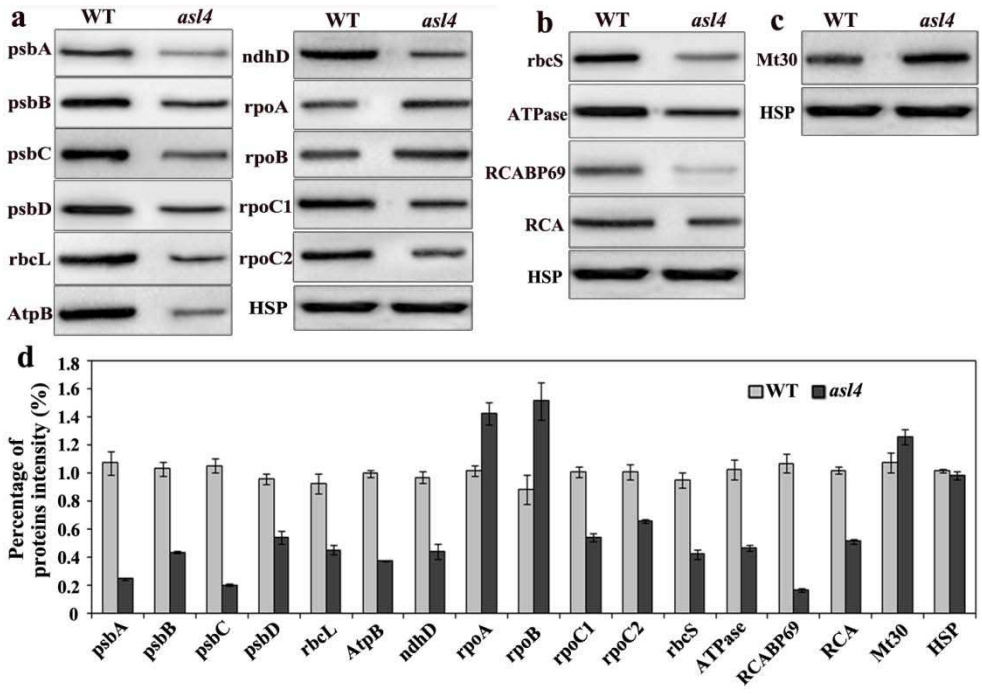

Figure 8 Levels of selected representative proteins. **a** Western blot analysis of plastid-encoded proteins in wild-type and *asl4* mutant seedlings at the L3 stage. **b** Western blot analysis of nuclear-encoded proteins in wild-type and *asl4* mutant seedlings at the L3 stage. **c** Western blot analysis of mitochondrial-encoded proteins in wild-type and *asl4* seedlings at the L3 stage. HSP 82 was used as internal control. **d** Quantification of the band intensity of the detected proteins in *asl4* mutant compare to wild type corresponding to **a**-**c**.

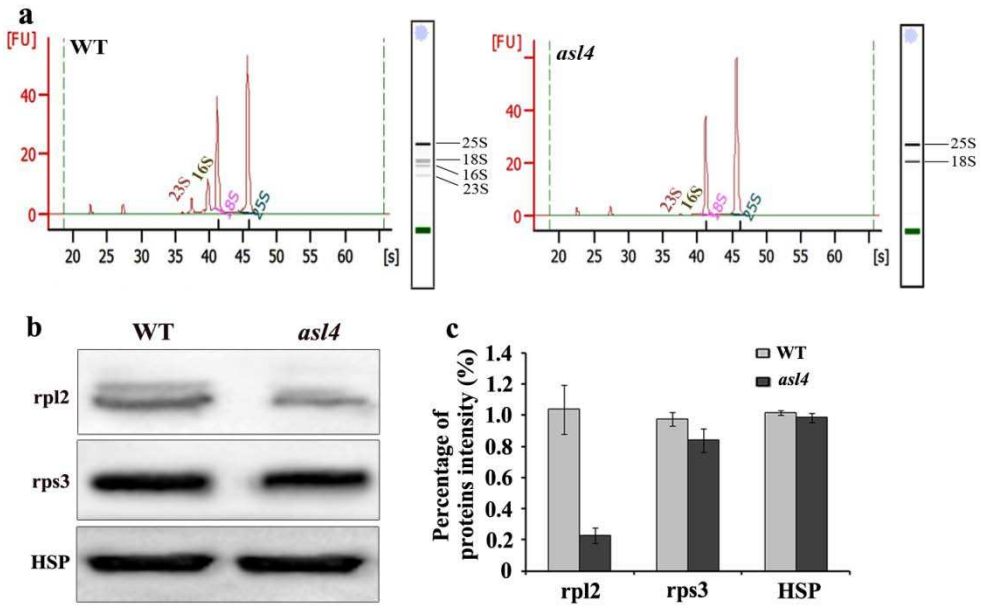

Figure 9 Plastid rRNA and ribosomal protein levels in wild-type and *asl4* mutant seedlings. **a** rRNA analysis of wild-type and *asl4* mutant seedlings at the L3 stage using an Agilent 2100 analyzer. **b** Western blot analysis of plastid ribosomal proteins in wild-type and *asl4* mutant seedlings at the L3 stage. HSP 82 was used as internal control. **c** Quantification of the band intensity of plastid ribosomal proteins corresponding to **b**.

Supplemental figure S1 Sequence alignment of the ASL4 and asl4 proteins. *Black underline* indicates the RNA binding domain.

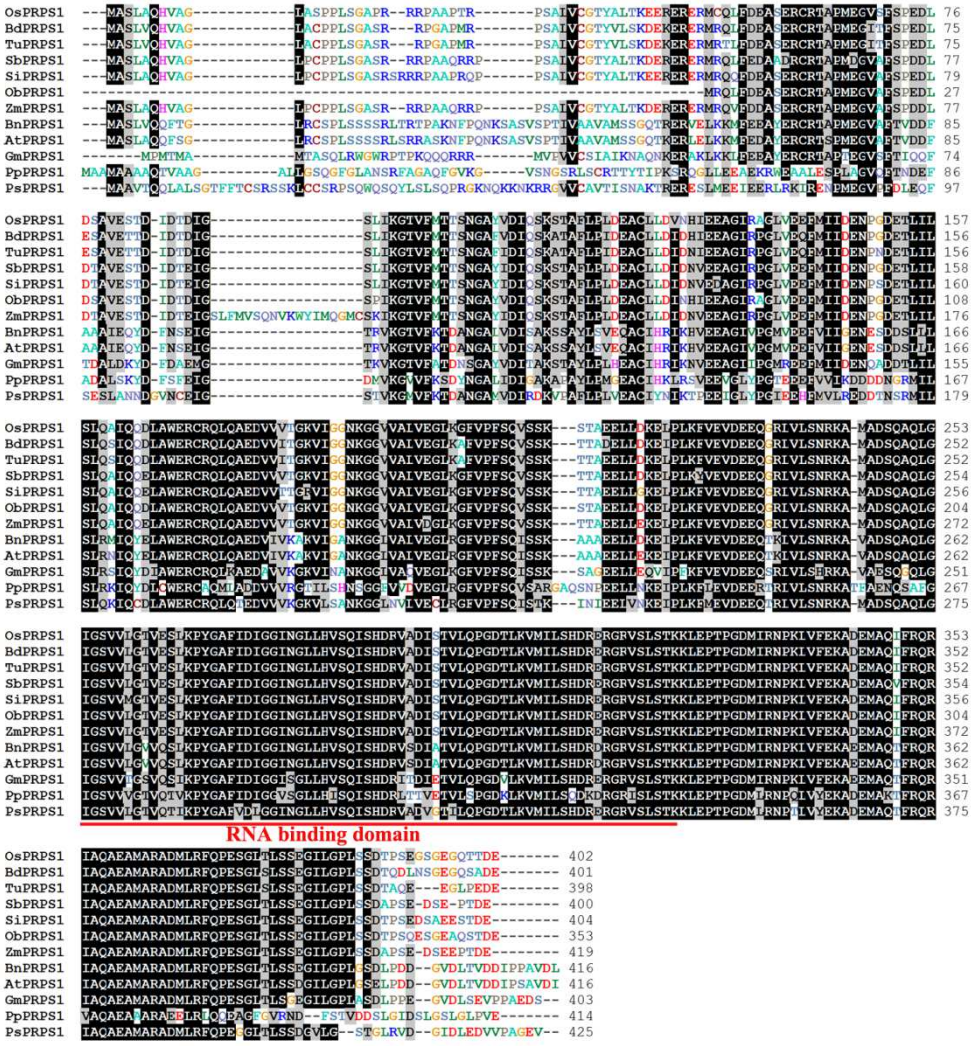

Supplemental figure S2 Sequence alignment of ASL4-related proteins. Sequences are for OsPRPS1 (OsASL4, *Oryza sativa*, LOC_Os03g20100), BdPRPS1 (*Brachypodium distachyon*, XP_003558047.1), TuPRPS1 (*Triticum urartu*, EMS48000.1), SbPRPS1 (*Sorghum bicolor*, XP_002465357.1), SiPRPS1 (*Setaria italic*, XP_004984580.1), ObPRPS1(*Oryza brachyantha*, XP_006649986.1), ZmPRPS1 (*Zea mays*, AQL07040.1), BnPRPS1 (*Brassica napus*, XP_013644063.1), AtPRPS1 (*Arabidopsis thaliana*, NP_850903.1), GmPRPS1 (*Glycine max*, NP_001348025.1), PpPRPS1 (*Physcomitrella patens*, XP_024386702.1), PsPRPS1 (*Picea sitchensis*, ABK25672.1). Red underline indicates the RNA binding domain.

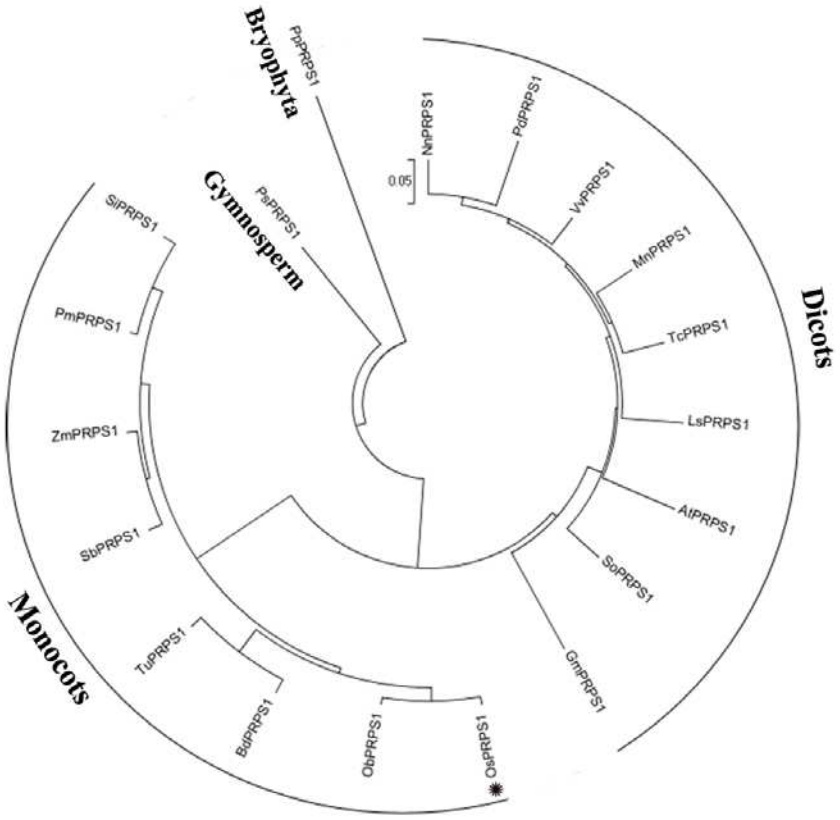

Supplemental figure S3 Phylogenetic analysis of ASL4 and its related proteins. OsPRPS1 is indicated a *black asterisk*. Sequences are for OsPRPS1 (OsASL4, *Oryza sativa*, LOC_Os03g20100), PpPRPS1 (*Physcomitrella patens*, XP_024386702.1), PsPRPS1 (*Picea sitchensis*, ABK25672.1). NnPRPS1(*Nelumbo nucifera*, XP_010270863.1), PdPRPS1(*Phoenix dactylifera*, XP_008781183.1), VvPRPS1(*Vitis vinifera*, XP_002280604.1), MnPRPS1(*Morus notabilis*, XP_010102913.1), TcPRPS1(*Theobroma cacao*, XP_017975185.1), LsPRPS1(*Lactuca sativa*, XP_023760774.1), AtPRPS1 (*Arabidopsis thaliana*, NP_850903.1), SoPRPS1(*Spinacia oleracea*, XP_021854510.1), GmPRPS1 (*Glycine max*, NP_001348025.1), ObPRPS1(*Oryza brachyantha*, XP_006649986.1), BdPRPS1 (*Brachypodium distachyon*, XP_003558047.1), TuPRPS1 (*Triticum urartu*, EMS48000.1), SbPRPS1 (*Sorghum bicolor*, XP_002465357.1), ZmPRPS1 (*Zea mays*, AQL07040.1), PmPRPS1(*Panicum miliaceum*, RLN42086.1), SiPRPS1 (*Setaria italic*, XP_004984580.1)

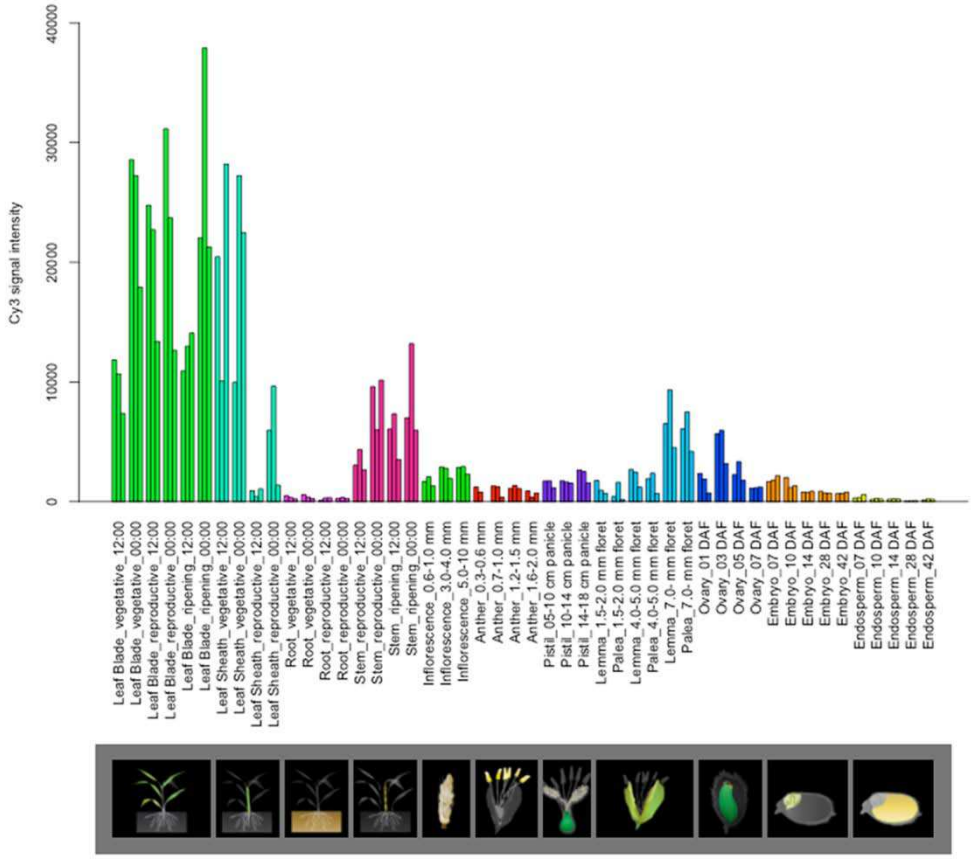

Supplemental figure S4 Expression profile of *ASL4* at different growth stages. Colors represent different tissues. Data were analyzed in RiceXPro, the rice expression profile database.

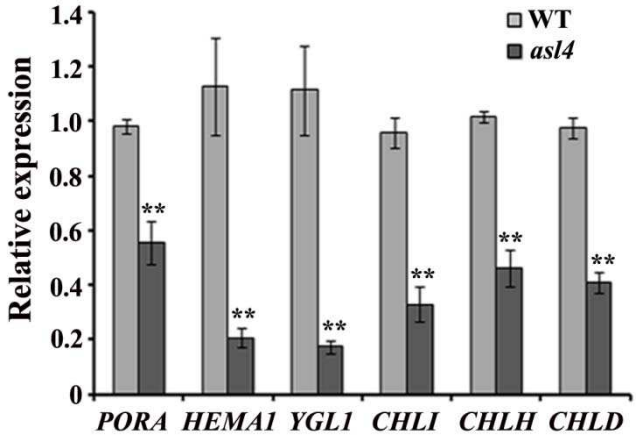

Supplemental figure S5 Expression levels of genes associated with Chlorophyll biosynthesis in wild-type and *asl4* mutant seedlings at the L3 stage. Data are means ± SD of three independent repeats. **, significance at $P = 0.01$ when analyzed by Student's *t* tests.

Figures

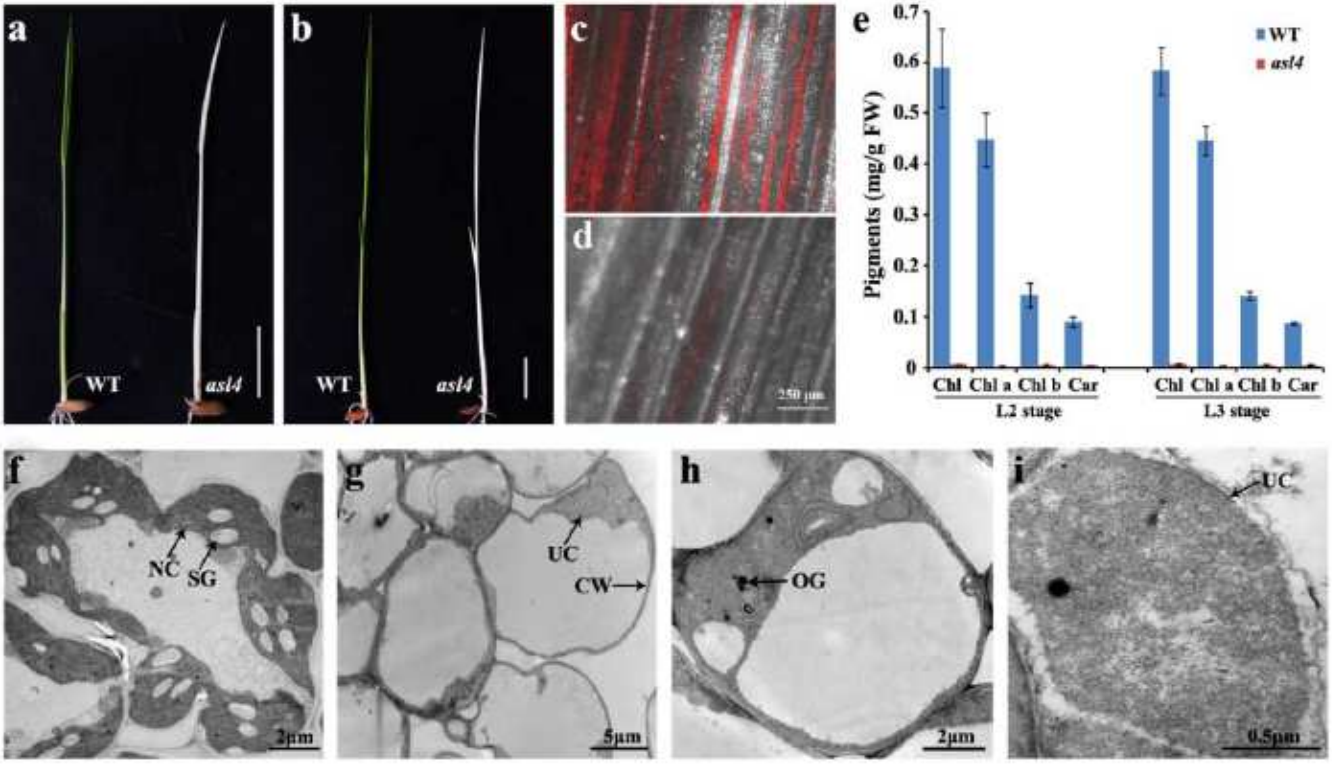

Figure 1

Phenotypic characteristics of the asl4 mutant. a Phenotype of wild type and the asl4 mutant at the L2 stage grown in the field. b Phenotype of wild type and the asl4 mutant at the L3 stage. Confocal microscope observation of chlorophyll-containing cells in seedlings of wild type (c) and the asl4 mutant (d). e Photosynthetic pigment determination in seedlings of wild type and asl4 mutant at the L2 and L3 stages. Values are means ± SD from three independent replicates. TEM observations of chloroplasts in wild type (f) and asl4 (g-i) seedlings at the L3 stage. NC normal chloroplast, SG starch granule, UC undifferentiated chloroplast, CW cell wall, OG osmiophilic plastoglobuli

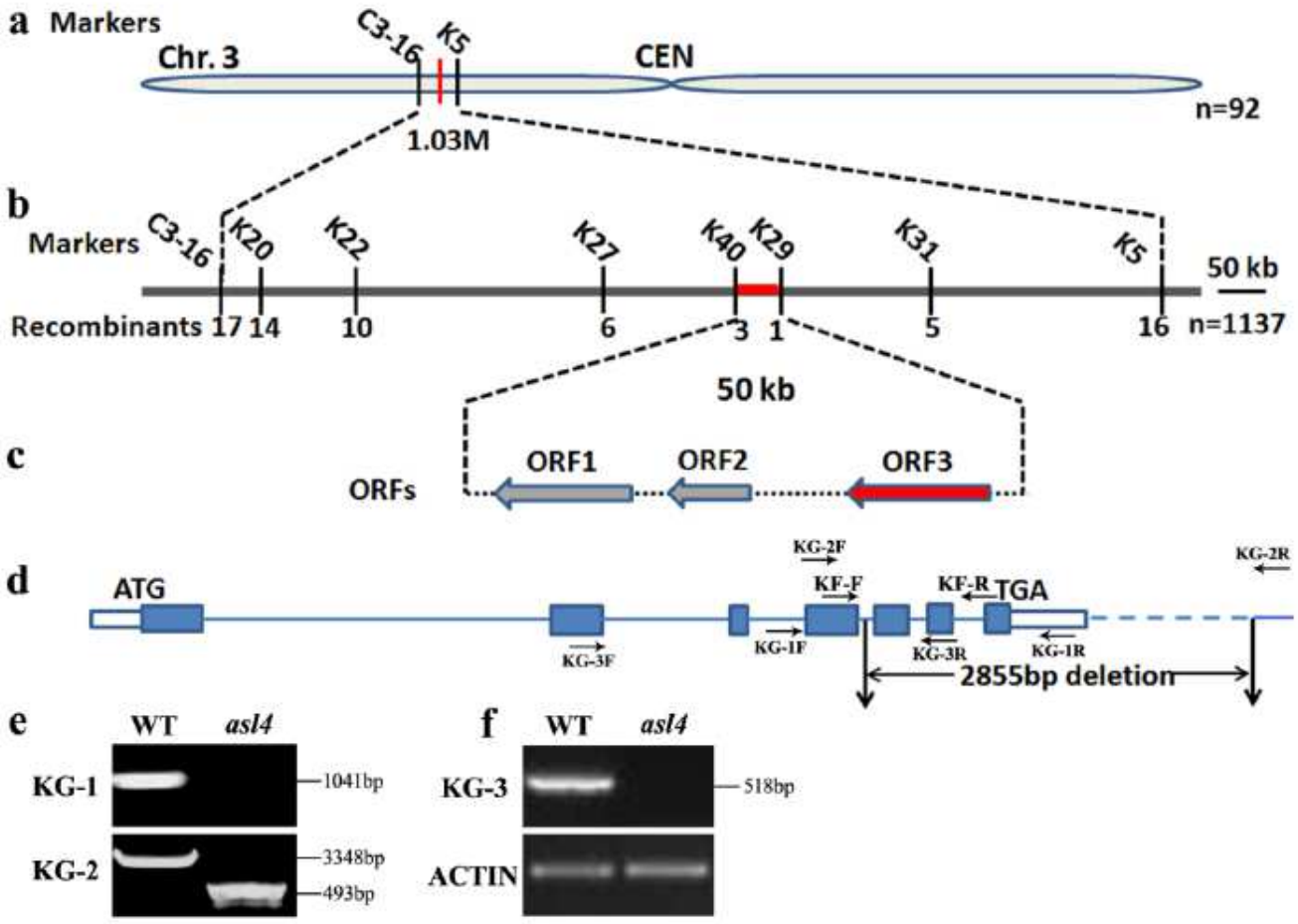

Figure 2

Map-based cloning of the ASL4 locus. a The ASL4 locus was initially mapped to a 1.03-Mb region between markers C3-16 and K5 on the short arm of chromosome 3. b ASL4 was fine-mapped to a 50-kb region between markers K40 and K29 using 1,137 F2 mutant seedlings. c Three ORFs were predicted in the region. d Structure of ASL4. ATG and TGA indicate start and stop codons. Blue boxes indicate exons and the lines between them indicate introns. White boxes represent the 5’ and 3’ UTR. The location of the 2,855-bp deletion in the asl4 allele is indicated. PCR identification of genomic DNAs (e) and cDNA (f) between wild type and asl4 mutant using primer pairs indicated in D. The actin gene was amplified as the control.

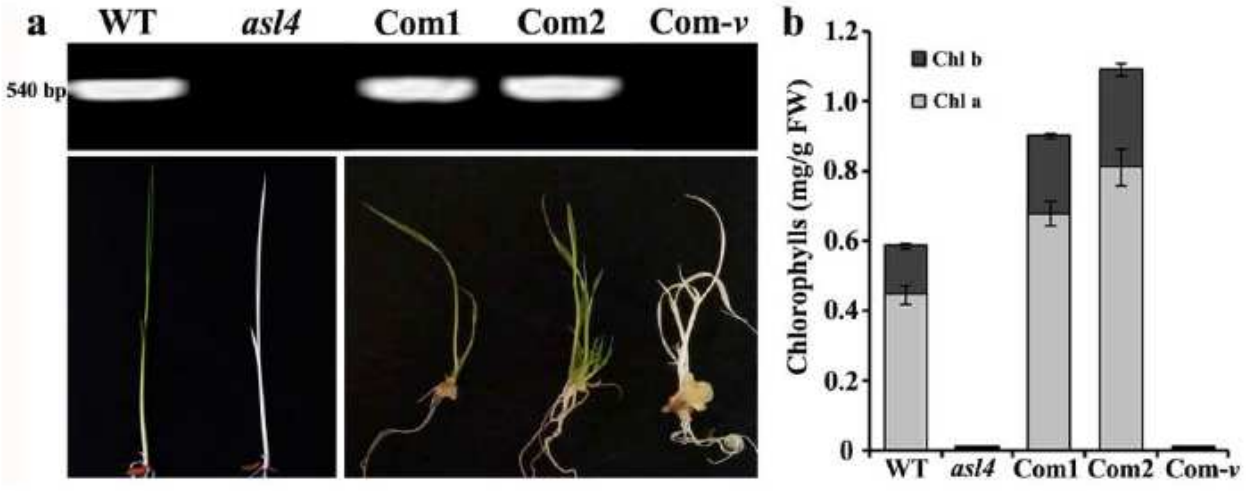

Figure 3

Complementation test of the asl4 mutation. a Phenotypes of wild type, asl4 mutant and transgenic plants. Primer KF indicated in figure 2D was used to distinguish positive and negative lines. b Chlorophyll contents of wild type, asl4 mutant and transgenic plants. Values are means ± SD from three independent repeats. Com1, Com2 and Com-v are two positive transgenic lines and transformation control with empty vector, respectively.

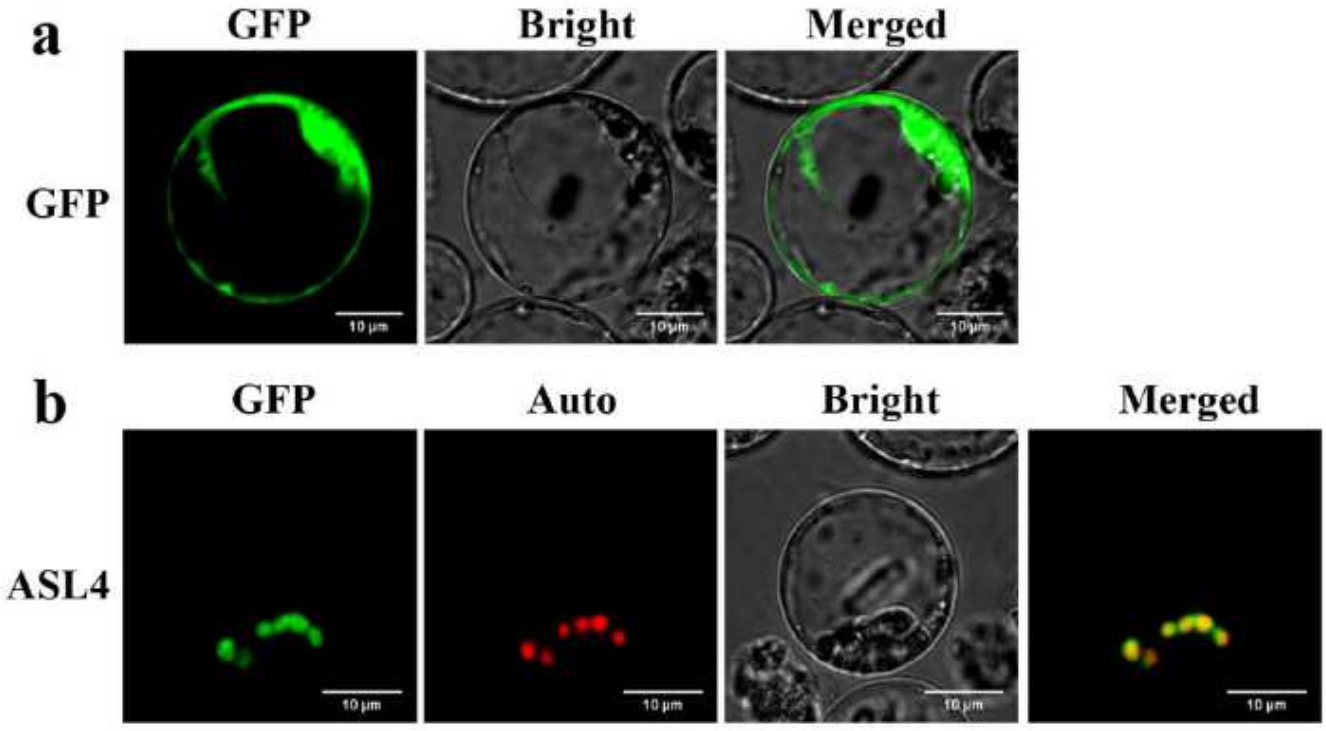

Figure 4

Subcellular location of ASL4 protein. a Free GFP signals in rice protoplasts. b ASL4-GFP signals were co-localized with chlorophyll autofluorescence in rice protoplasts. GFP, GFP signals of free GFP and ASL4; Auto, chlorophyll autofluorescence; Bright, bright field; Merged, merged images.

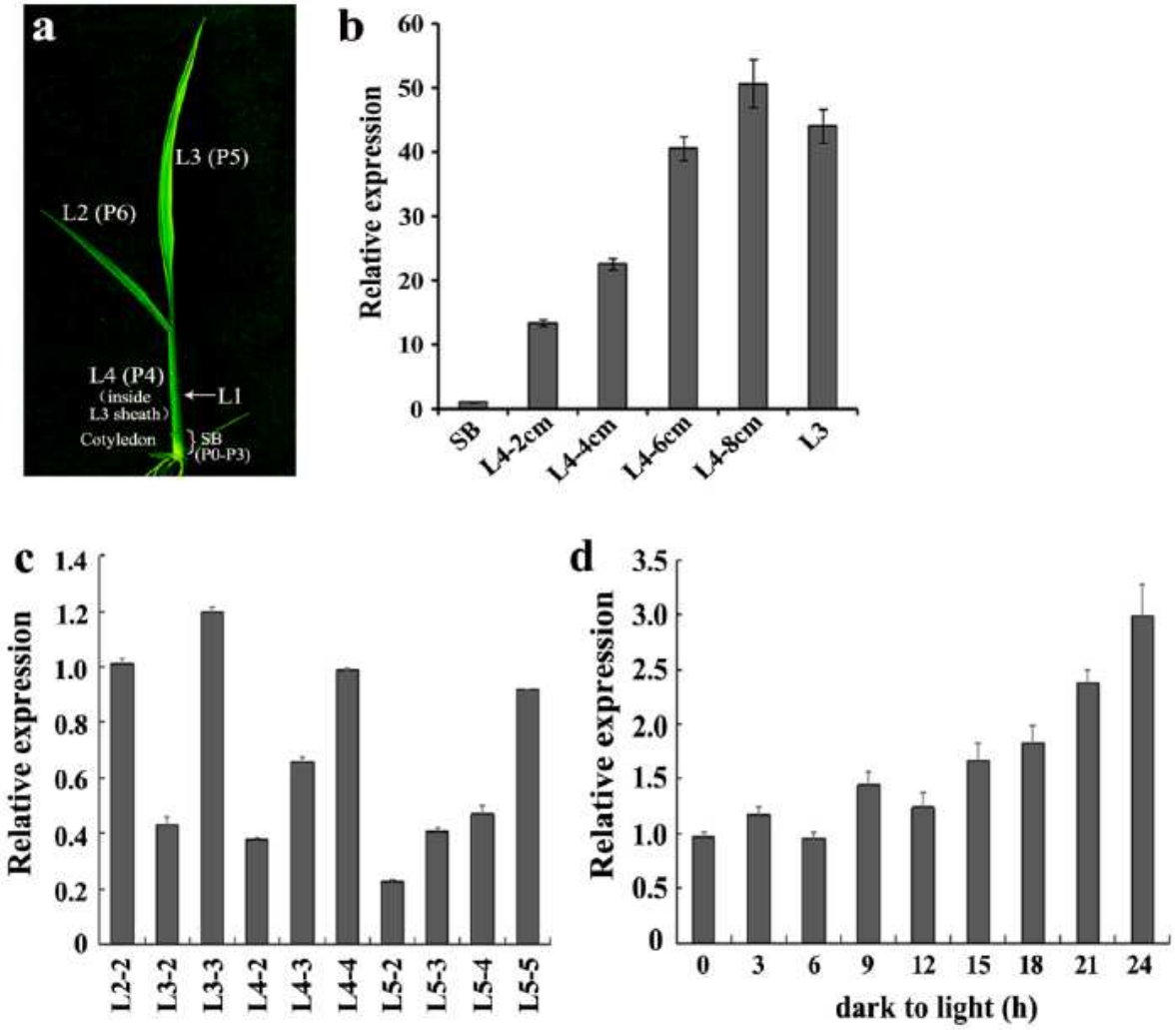

Figure 5

Expression analysis of ASL4. a Diagram of a L3 stage seedling when leaf 3 is fully expanded. SB (shoot base) indicates a 5 mm piece from the bottom of the shoot. L1-L4 represent leaves 1 to 4 in the L3 stage seedling. P0-P6 represent the developmental stages of leaf formation. b Expression of ASL4 in different wild-type sections at the L3 stage seedling from the paddy field. L4-2 cm, 4 cm, 6 cm and 8 cm indicate the length of the L4 leaf. c Expression levels of ASL4 in wild-type leaves at different stages. For example, L2-2 represent leaf 2 of a L2 stage seedling, L3-2 represent leaf 2 of a L3 stage seedling. d Expression analysis of ASL4 during light-induced greening of wild-type seedlings. Wild-type seedlings were exposed to light for 3h, 6h, 9h, 12h, 15h, 18h, 21h and 24h after 10 days of growth at 30□in darkness. The ubiquitin gene was used as internal control. Values are means ± SD from three independent replicates.

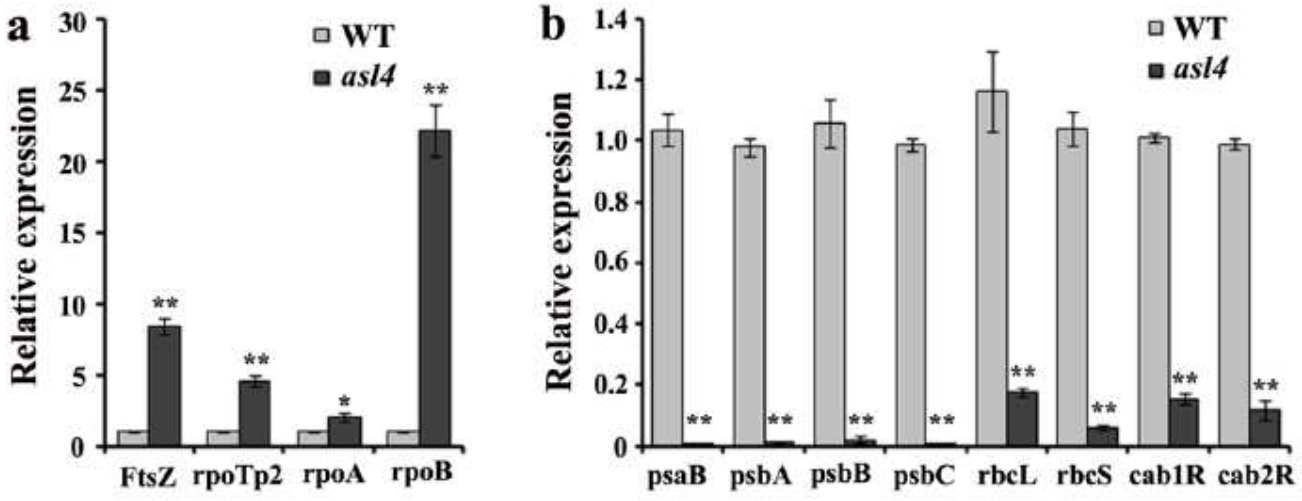

Figure 6

Expression levels of genes involved in chloroplast biogenesis. Expression levels of genes associated with the first and second (a) and third (b) steps of chloroplast biogenesis in wild-type and asl4 mutant seedlings at the L3 stage. Data are means ± SD of three independent repeats. ** and *, indicate significance at P = 0.01 and P = 0.05, respectively, by Student's t tests.

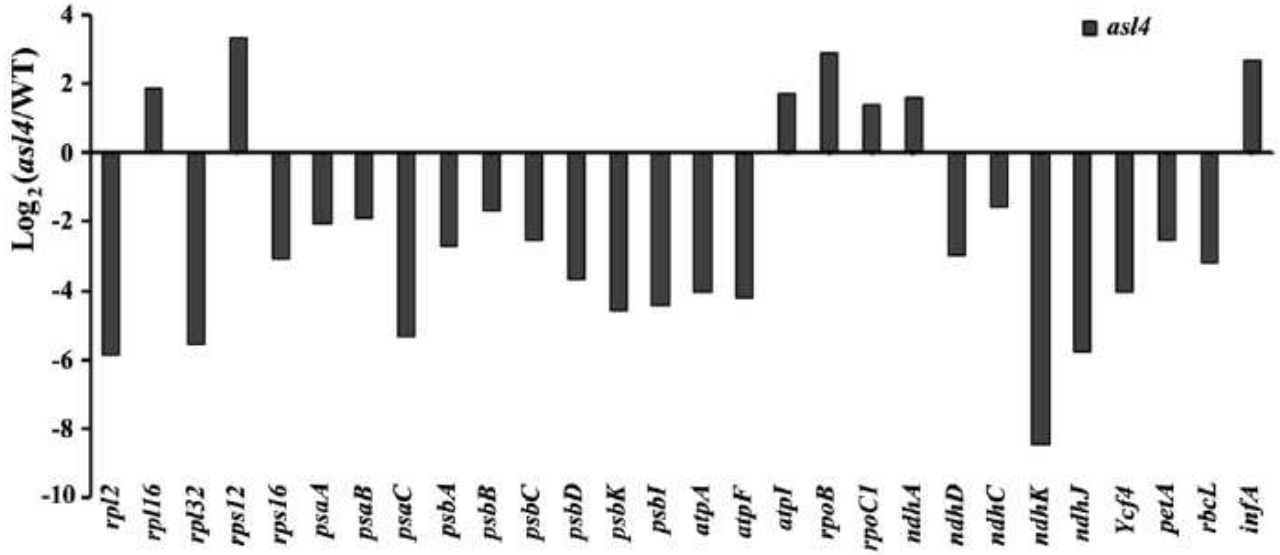

Figure 7

Transcripts of plastid-encoded genes detected by transcriptome analysis. Total RNA was isolated from wild-type and asl4 mutant seedlings at the L3 stage and reverse-transcribed by random hexamer primers. The library was constructed and sequenced with an Illumina HiSeq 2000. Log2 (asl4/WT) indicates the log2 ratio of mRNA levels in asl4 mutant compared to wild type.

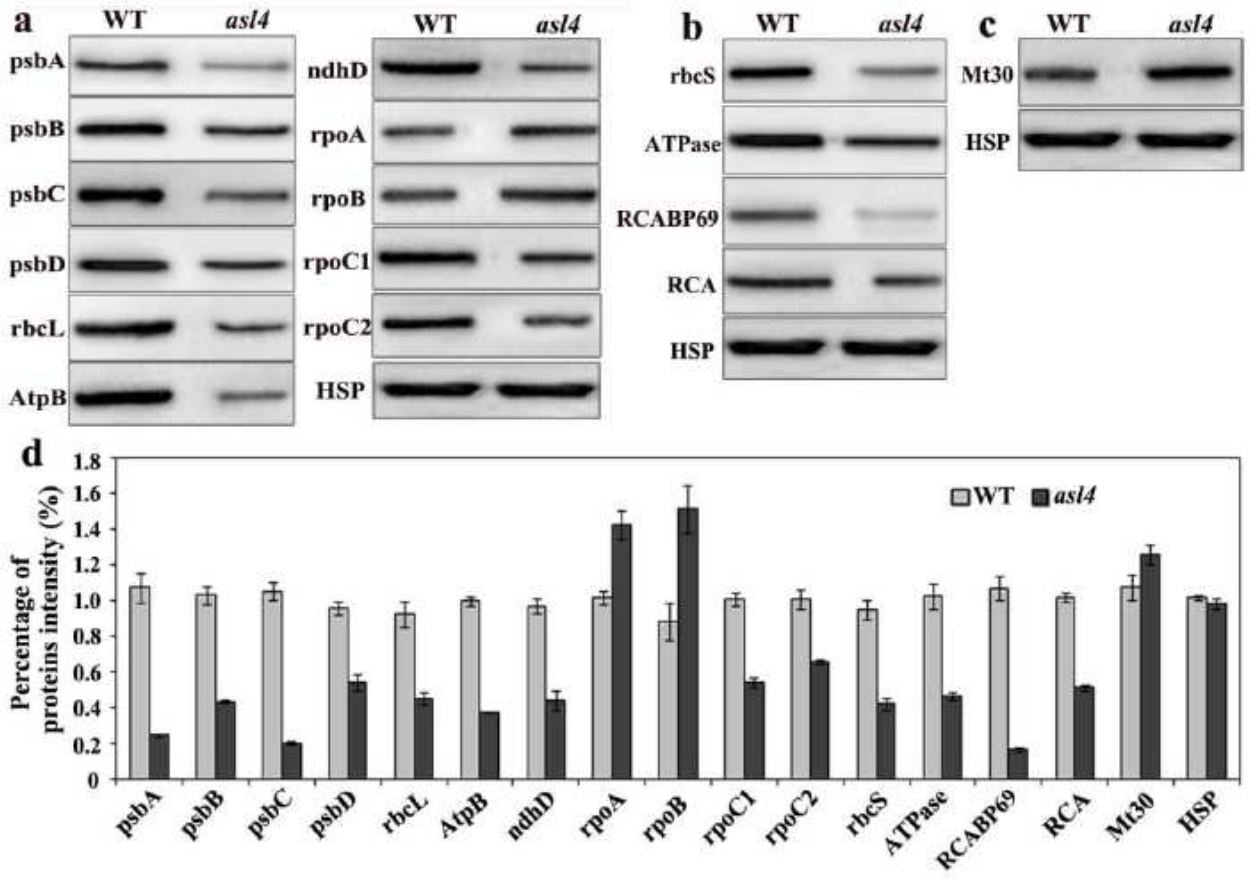

Figure 8

Levels of selected representative proteins. a Western blot analysis of plastid-encoded proteins in wild-type and asl4 mutant seedlings at the L3 stage. b Western blot analysis of nuclear-encoded proteins in wild-type and asl4 mutant seedlings at the L3 stage. c Western blot analysis of mitochondrial-encoded proteins in wild-type and asl4 seedlings at the L3 stage. HSP 82 was used as internal control. d Quantification of the band intensity of the detected proteins in asl4 mutant compare to wild type corresponding to a-c.

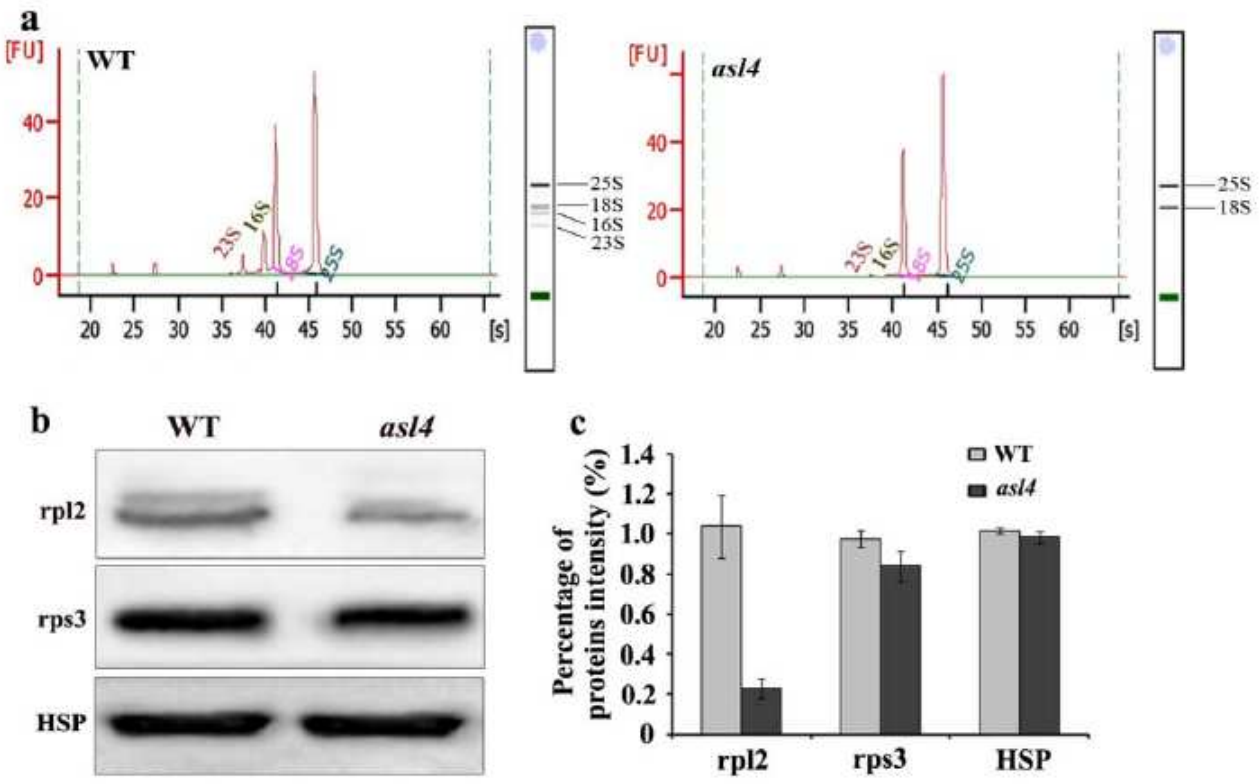

Figure 9

Plastid rRNA and ribosomal protein levels in wild-type and asl4 mutant seedlings. a rRNA analysis of wild-type and asl4 mutant seedlings at the L3 stage using an Agilent 2100 analyzer. b Western blot analysis of plastid ribosomal proteins in wild-type and asl4 mutant seedlings at the L3 stage. HSP 82 was used as internal control. c Quantification of the band intensity of plastid ribosomal proteins corresponding to b.

Supplementary Files

This is a list of supplementary files associated with this preprint. Click to download.

- TableS1.pdf